microPublication BIOLOGY

11/10/2026 - *Open Access*

βtubulin>GCaMP6s and βtubulin>H2B-GCaMP6s-T2A-mCherry enable pan-neuronal Ca^{2+}imaging and more accurate measuring neural activity in *Ciona robusta*

Yuta Yoshino[1], Manami Doi[2], Kohji Hotta[2§]

[1]Shibuya Senior High School, Tokyo, 13, Japan

[2]Department of Biosciences and Informatics, Faculty of Science and Technology, Keio University, Tokyo, 13, Japan

[§]To whom correspondence should be addressed: khotta@keio.jp

Abstract

The βtubulin promoter of *Ciona robusta* has been widely used as a pan-neuronal marker, but it has rarely been applied to imaging neural activity itself. In this study, two Ca^{2+}imaging constructs were developed using this promoter: βtubulin>GCaMP6s and βtubulin>H2B-GCaMP6s-T2A-mCherry. Larvae carrying the former showed fluorescence throughout the nervous system, while in the latter, GCaMP6s was co-expressed in the nucleus and mCherry in the somata, enabling ratiometric correction using mCherry as a calcium-independent reference signal. With both constructs, the excitation of neurons could be visualized. These results demonstrate that the two constructs are suitable tools for pan-neuronal imaging in *C. robusta*.

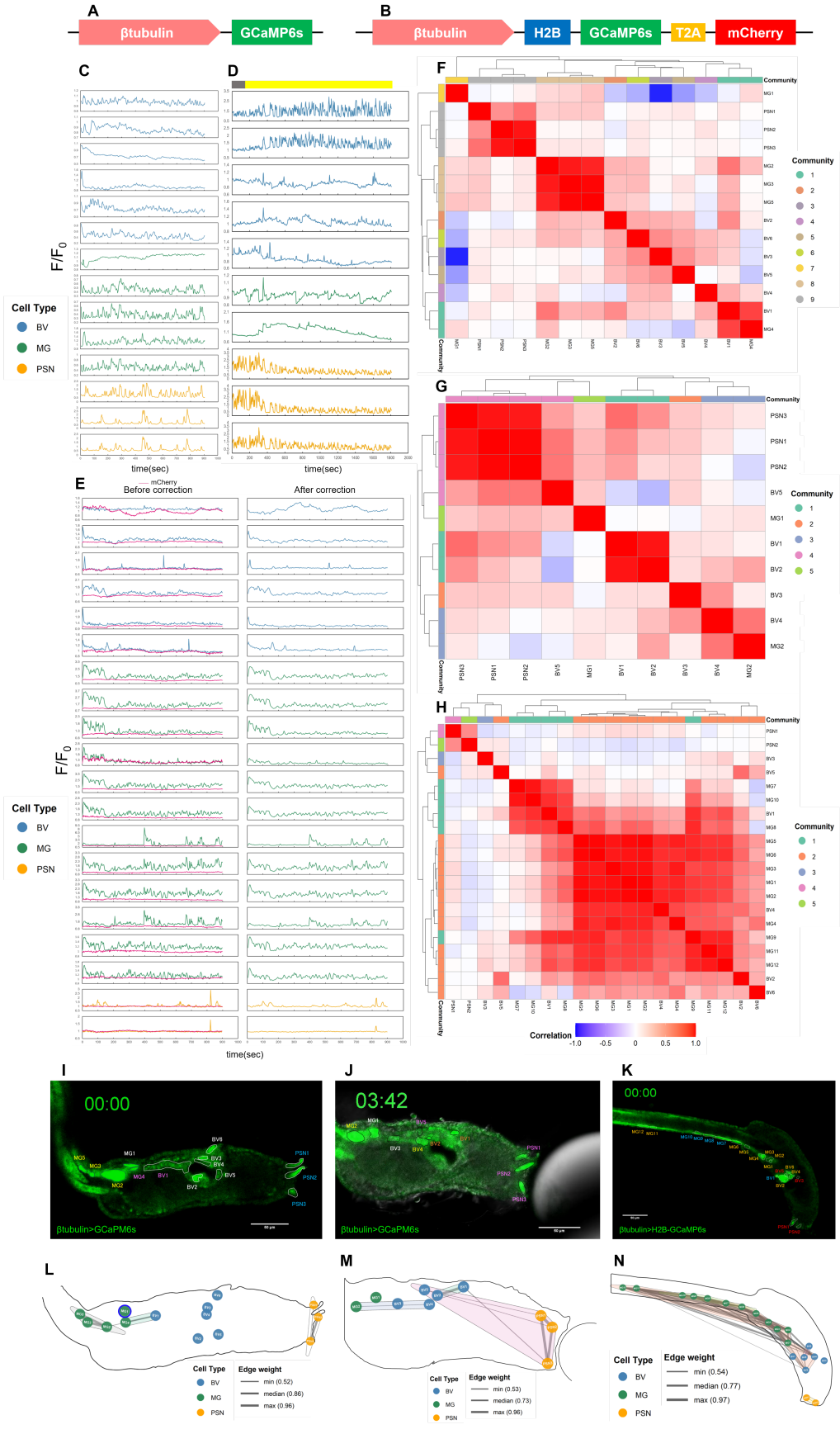


Figure 1. *C. robusta* observed using βtubulin>GCaMP6s and βtubulin>H2B-GCaMP6s-T2A-mCherry, and analysis results:

(A) Schematic diagram of βtubulin>GCaMP6s. In reality, it is a circular plasmid.

(B) Schematic diagram of βtubulin>H2B-GCaMP6s-T2A-mCherry. In reality, it is a circular plasmid.

(C) A figure shows neural activity measured without mechanical stimulation by using βtubulin>GCaMP6s. Cell types are color-coded and numbered in order from top to bottom (e.g., BV1, BV2, ... MG1, MG2, ... PSN1, PSN2, ...). Please refer to the extended data section for details on the actual observations and the locations of each cell.

(D) A figure shows neural activity measured while the papillae of a larva were stimulated with a glass needle. Stimulation was applied at approximately 130 s after the start of the measurement. The gray area indicates the period before stimulation, and the yellow area indicates the period during stimulation. Cell types are color-coded and numbered in order from top to bottom (e.g., BV1, BV2, ... MG1, MG2, ... PSN1, PSN2, ...). Please refer to the extended data section for details on the actual observations and the locations of each cell.

(E) A figure shows neural activity measured without mechanical stimulation by using βtubulin. Cell types are color-coded and numbered in order from top to bottom (e.g., BV1, BV2, ... MG1, MG2, ... PSN1, PSN2, ...). Please refer to the extended data section for details on the actual observations and the locations of each cell.

(F) A figure shows the similarity of intensity fluctuations in figure 1C by using CalciumNetExploreR (CNER). Nine communities were detected, including isolated ones. BV1, BV4, and MG4 belong to communities 1 and 4. BV3 and BV5 belong to communities 3 and 5. BV2 and BV6 belong to Communities 2 and 6. MG1 belongs to community 7. MG2, MG3, and MG5 belong to Community 8. PSN1, PSN2, and PSN3 belong to Community 9. Negative correlations were observed between MG1 and BV1 to BV6, and were particularly pronounced with BV3.

(G) A figure shows the similarity of intensity fluctuations in figure 1D by using CNER. Five communities were detected, including isolated ones. BV1 and BV2 belong to community 1. BV3, BV4, and MG2 belong to communities 2 and 3. PSN1, PSN2, PSN3, BV5, and MG1 belong to communities 4 and 5. Negative correlations were observed between MG2 and BV5, PSN2, and PSN1; between BV5 and BV1, BV2, and MG2; and between MG1 and BV3, and were particularly pronounced between MG2 and PSN2 and between BV5 and BV2.

(H) A figure shows the similarity of intensity fluctuations in figure 1E by using CNER. Five communities were detected, including isolated ones. Data subjected to ratiometric correction were used for the analysis, and the following formula was used for the correction: $F = GCaMP6s / mCherry$. BV1 and MG7 to MG10 belong to community 1. BV2, BV4, BV6, and MG1 to MG6, MG11, and MG12 belong to community 2. BV3, BV5, PSN1, and PSN2 belong to communities 3, 4, and 5. MG9 appeared to belong not only to community 1 but also to community 2.

(I) An image showing the names and locations of the cells labeled in figures 1C and 1F. Color-coded by community but the colors themselves are not significant.

(J) An image showing the names and locations of the cells labeled in figures 1D and 1G. Color-coded by community but the colors themselves are not significant.

(K) An image showing the names and locations of the cells labeled in figures 1E and 1H. Color-coded by community but the colors themselves are not significant.

(L) A model of figure 1I. Each community is color-coded but the colors themselves are not significant. The connections between the nodes are represented by lines. The threshold is set to 0.5, and the thicker the line, the stronger the correlation.

(M) A model of figure 1J. Each community is color-coded but the colors themselves are not significant. The connections between the nodes are represented by lines. The threshold is set to 0.5, and the thicker the line, the stronger the correlation.

(N) A model of figure 1K. Each community is color-coded but the colors themselves are not significant. The connections between the nodes are represented by lines. The threshold is set to 0.5, and the thicker the line, the stronger the correlation.

Description

The larva of *C. robusta* has a central nervous system (CNS) composed of 177 neurons, the notochord, the neural tube, and the brain vesicle (Ryan et al., 2016). Whereas the notochord develops into the vertebral column in vertebrates, in *C. robusta* it is known to disappear during metamorphosis together with the regression of the larval organs. The CNS of *C. robusta* contains the otolith (OT), the ocellus (OC), and photoreceptors (PR). These structures are called the brain vesicle (BV). Also, it has the peripheral interneurons (PNIN), motor neurons (MN), the Ascending motor ganglion neurons (AMG) and the motor ganglion interneurons (MGIN) which are involved in movement of the tail. These are called the motor ganglion (MG). It has peripheral sensory neurons (PSN) which detect stimuli from the papillae and convey them to BV. (Olivo et al., 2021; Ryan et al., 2016).

For imaging neural activity in *C. robusta* larvae, constructs employing the prohormone convertase 2 (PC2) promoter has been used. However, this construct carries limitations. Although PC2 has been widely used as a pan-neuronal marker

(Sekiguchi et al., 2007), its expression is not restricted to neurons and extends to a diverse range of peripheral peptidergic cells outside the nervous system (Osugi et al., 2020). This calcium signals thereby obtained inevitably contain extensive background arising from non-neural cells in addition to neural origin. The βtubulin>GCaMP6s construct generated in the present study overcomes the limits of above construct in principle (Fig. 1A). The Ci-βtubulin promoter was originally discovered as a marker of neural cell differentiation in *C. robusta* larvae (Miya and Satoh, 1997), and it has been used as a pan-neuronal marker for various purposes (Hamada et al., 2011; Horie et al., 2011; Hozumi et al., 2015; Kusakabe et al., 2004). However, few studies have used it for the purpose of imaging neural activity itself. Thus, βtubulin>GCaMP6s is superior to those having been used in that they enable comprehensive measurement of activity throughout the nervous system while excluding non-neural background signals.

As the experiment progressed, although βtubulin>GCaMP6s reports calcium signals in axons and neuropil in addition to cell bodies, we found it was difficult to isolate signals from individual somata in densely packed regions, and larval movement during observation occurred fluorescence fluctuations unrelated to neural activity. To deal these issues, βtubulin>H2B-GCaMP6s-T2A-mCherry was constructed (Fig. 1B) in which GCaMP6s is confined to the nucleus and mCherry is co-expressed in the somata by the self-cleaving peptide T2A (de Felipe et al., 2006; Donnelly et al., 2001; Liu et al., 2017). T2A is a self-cleaving peptide that has been used as a means of co-expressing multiple proteins of interest from a single construct (Totsuka and Hotta, 2026). Concentrating GCaMP6s in the nucleus eliminates overlapping axonal signals and allows individual somata to be identified clearly as ROIs. Because mCherry fluorescence is independent of calcium concentration, its fluctuations can be seen as motion artifacts or defocusing. Thus, we can use mCherry fluorescence as a reference signal for ratiometric correction of the GCaMP6s signal. This approach has been used to reduce motion artifacts in calcium imaging (Nguyen et al., 2016; Venkatachalam et al., 2016).

In this study, βtubulin>GCaMP6s and βtubulin>H2B-GCaMP6s-T2A-mCherry, based on the Ci-βtubulin promoter, were newly generated. As described in before section, these are considered to overcome in principle the limits of the constructs having been used. Indeed, βtubulin>GCaMP6s's fluorescence was observed at a broad range of the nervous system (Figs. 1C, 1D, 1F, 1G, 1I, 1J, 1L, 1M, Extended data). This construct can therefore be regarded as a tool suitable for pan-neuronal imaging in *C. robusta* larvae that surpasses existing constructs in simultaneously satisfying neural specificity by excluding non-neural signals and comprehensiveness by visualizing the entire nervous system. Its novelty is achieving with a single construct the two requirements of specificity and comprehensiveness, which are often difficult to reconcile. However, some nervous systems were rarely observed while they should be more observed, and room for further improvement of the constructs remains. In βtubulin>H2B-GCaMP6s-T2A-mCherry, localizing GCaMP6s to the nucleus by fusing with H2B eliminated the overlapping signals of axonal origin and enable us to identify individual neuronal somata obviously as ROI. Because GCaMP6s's fluorescence was localized in the nucleus, the definition of ROIs is facilitated, which suited the aim of this study of tracking multiple cells at the same time. You can also choose between the two types of constructs depending on the subject you want to observe (e.g. if you want to see the axon in addition to the somata, you can use βtubulin>GCaMP6s and if you want to see specific nervous system clearly, you can use βtubulin>H2B-GCaMP6s-T2A-mCherry).

The principal feature of βtubulin>H2B-GCaMP6s-T2A-mCherry lies in its design, in which nuclear-localized GCaMP6s and cytoplasm-specific mCherry are co-expressed. Because larvae of *C. robusta* move actively and the specimen shift out of the focal plane, the fluorescence of GCaMP6s contains artifacts from defocusing in addition to changes in calcium concentration. Since the fluorescence of mCherry does not depend on calcium concentration, its fluctuations can be regarded as components attributable to defocusing (Figs. 1E, 1H, 1K, 1N, Extended data). By using mCherry, which is always co-expressed at a constant ratio in the same cell, these artifacts can be corrected in the GCaMP6s signal. This procedure is expected to separate genuine excitation of neural structures by increasing calcium concentration from motion artifacts and thereby to enhance the reliability of the analysis. Using a dual-color design makes a core advantage of this construct in that it not only facilitates ROI identification but also provides a basis for quantitative noise correction. In the network analysis using CNER, some communities were detected from the correlation structure of the fluorescence time series of each ROI. Also, it demonstrated that the community structure differed according to the presence or absence of stimulation (Figs. 1C, 1E, 1F, 1H, 1I, 1K, 1L, 1N). Sample of Figs 1D, 1G, 1J and 1M reacts to mechanical stimulation with a glass needle, and Samples of figs 1C, 1E, 1F, 1H, 1I, 1K, 1L and 1N had fluorescence even without mechanical stimulation. it is thought that this is because that these samples react to laser light used for observation. These results suggest that the larva of *C. robusta's* CNS may have a functional modular structure superimposed upon the known connectome (Ryan et al., 2016). In particular, the finding that MG1 showed negative correlations with multiple ROIs (Figs. 1C, 1F, 1I, 1L) may reflect inhibitory connectivity. Taken together, this study demonstrates that this approach captures not only the visualization of neurons but also the fact that different neuronal populations are excited depending on the type of stimulus at the level of functional connectivity. However, since the ROIs where GCaMP6 and mCherry are expressed differ in this construct, it may not be suitable for completely eliminating noise due to the differences in concentration of fluorescence between the nucleus and the cytoplasm. As a future challenge, to achieve more accurate measurements, we could develop a construct that localizes non-calcium-derived signals within the nucleus while keeping the construct length short.

Methods

Construction of βtubulin>GCaMP6s

Genomic DNA was extracted from the eggs and sperm of *C. robusta* using NucleoBond HMW DNA (Takara Bio). The nucleotide sequence of the Ci-βtubulin promoter was identified on the basis of the Ghost Database compiled by the Satoh group, Laboratory of Developmental Biology, Department of Zoology, Graduate School of Science, Kyoto University. The *C. robusta* used in the present study were obtained from the National BioResource Project (NBRP) through the Shimoda Marine Research Center, University of Tsukuba; the Graduate School of Science, Kyoto University; and the Misaki Marine Biological Station, Graduate School of Science, The University of Tokyo.

The βtubulin>GCaMP6s construct was generated by nested PCR. In the first step (KOD One PCR), the βtubulin promoter region was amplified from genomic DNA (primers: forward 5'-GGAGTCCAGATAAACTTGGA-3', reverse 5'-TAGCTCCGATTTGGTTGCCG-3'). In the second step (HiFi PCR), the insert was amplified from the product of the first step (primers: forward 5'-ATGGGTTCTCATCAT-3', reverse 5'-GACTCTAGAGGATCC-3'), and the vector was amplified from a PC2>GCaMP6s plasmid previously prepared in our laboratory (primers: forward 5'-GACTCTAGAGGATCCGATCAAGCACTGAGG-3', reverse 5'-CATCTGCAAGCTGGCCATGGGTTCTCATC-3'). The products of each step were verified by agarose gel electrophoresis and then purified from the gel using the Wizard SV Gel and PCR Clean-Up System (Promega). The purified insert and vector fragments were joined by homologous recombination using In-Fusion HD Enzyme Premix (Takara Bio) to construct the βtubulin>GCaMP6s plasmid. The sequence of the purified construct was verified by Sanger sequencing (Azenta Life Sciences) and by ClustalW alignment (Thompson et al., 1994).

Construction of βtubulin>H2B-GCaMP6s-T2A-mCherry

In order to express GCaMP6s localized to the nucleus of neurons together with mCherry localized to the cytoplasm, the βtubulin>H2B-GCaMP6s-T2A-mCherry construct was generated. The insert was amplified from PC2>H2B-GCaMP6s-T2A-mCherry, which had been prepared in our laboratory (forward: 5'-ATCTGCAAGCTGGCCATGGTTGCATCCAAA-3', reverse: 5'-GCTCAGCTGGAATTCTTACTTGTACAGCTC-3'), and the vector was amplified from the βtubulin>GCaMP6s plasmid described in the before section (forward: 5'-GAATTCCAGCTGAGC-3', reverse: 5'-GGCCAGCTTGCAGAT-3'), each serving as template for KOD One PCR. All subsequent procedures, from purification onward, were performed as described in the before section.

Electroporation into *Ciona robusta* eggs

DNA constructs were introduced into fertilized eggs by electroporation using a Gene Pulser Xcell system (Bio-Rad). After introduction, the fertilized eggs were distributed into gelatin-coated dishes and incubated at 20°C.

Fluorescence imaging

Swimming larvae were immobilized by adhering them to the bottom of Poly-L-Lysine (PLL)-coated dishes in order to restrict their movement. For imaging of neural activity, a confocal laser scanning microscope (Olympus FLUOVIEW FV4000) was used with a 20× objective lens. Mechanical stimulation was delivered to the papillae of larvae immobilized on PLL-coated dishes using a glass needle fabricated with a PC-10 puller (NARISHIGE) and mounted on a motorized micromanipulator (NARISHIGE MM-89). All observations were performed at a room temperature of 20°C.

Image processing with Fiji

The acquired fluorescence images were processed using the open-source image analysis platform Fiji (Schindelin et al., 2012), and time-series data of fluorescence intensity were extracted for each neuronal ROI. Data subjected to ratiometric correction were used for the analysis, and the following expression was used for the correction: F = GCaMP6s / mCherry

Analysis with CalciumNetExploreR (CNER)

Network diagrams and heatmaps representing functional connectivity between neurons were generated using CNER (Lenci and Sieger, 2025), an R package dedicated to network analysis of calcium imaging data. The extracted fluorescence time series of each ROI were normalized to the interval [0, 1] by min–max normalization, and a correlation matrix based on Pearson's product-moment correlation coefficient was calculated in order to evaluate the similarity of activity patterns between cells. Community detection was then performed on the resulting data using the Louvain method (Blondel et al., 2008). Pairs with a correlation coefficient of 0.5 or greater were subsequently regarded as edges, and a neural network diagram was constructed (Extended data). In drawing the network diagram, nodes were color-coded according to cell type and the line width of each edge was made proportional to the strength of the connection. Communities were further enclosed together so as to emphasize the subgraph structure visually. The correlation matrix was additionally visualized as a heatmap (Figs. 1F,1G and 1H). A red–blue gradient was used for the color scale, and a dendrogram was appended by hierarchical clustering using the group average method. Community information was also displayed in a sidebar as row and column annotations so that the cluster structure could be grasped intuitively.

Reagents

Construct	PCR protocol	Sequence	Primer detail
βtubulin>GCaMP6s	KOD One PCR	5'-GGAGTCCAGATAAACTTGGA-3'	Forward
βtubulin>GCaMP6s	KOD One PCR	5'-TAGCTCCGATTTGGTTGCCG-3'	Reverse
βtubulin>GCaMP6s	HiFi PCR	5'-ATGGGTTCTCATCAT-3'	Insert forward
βtubulin>GCaMP6s	HiFi PCR	5'-GACTCTAGAGGATCC-3'	Insert reverse
βtubulin>GCaMP6s	HiFi PCR	5'-GACTCTAGAGGATCCGATCA AGCACTGAGG-3'	Vector forward
βtubulin>GCaMP6s	HiFi PCR	5'-CATCTGCAAGCTGGCCATGGGTTCTCATC-3'	Vector reverse
βtubulin>H2B-GCaMP6s-T2A-mCherry	KOD One PCR	5'-ATCTGCAAGCTGGCCATGGT TGCATCCAAA-3'	Insert forward
βtubulin>H2B-GCaMP6s-T2A-mCherry	KOD One PCR	5'-GCTCAGCTGGAATTCTTACT TGTACAGCTC-3'	Insert reverse
βtubulin>H2B-GCaMP6s-T2A-mCherry	KOD One PCR	5'-GAATTCCAGCTGAGC-3'	Vector forward
βtubulin>H2B-GCaMP6s-T2A-mCherry	KOD One PCR	5'-GGCCAGCTTGCAGAT-3'	Vector reverse

Acknowledgements: The authors are deeply grateful to Dr. Mika Tanaka, Project Lecturer, Department of Chemistry, School of Medicine, Keio University; Dr. Hiroyoshi Inoue, Professor, Department of Chemistry, School of Medicine, Keio University; the members of the Laboratory of Evolutionary Developmental Biology and Neuroinformatics; all those involved in the GSC program; and the staff of the Japan Science and Technology Agency.

Extended Data

Description: This video shows observations the specimens described in figures 1C, 1F, 1I and 1L using a confocal laser scanning microscope (βtubulin>GCaMP6s). GCaMP6s was confirmed to be expressed across a broad range of the nervous system extending from the PSN to the BV and MG.. Resource Type: Audiovisual. File: 260203_no.mp4. DOI: 10.22002/aygxx-h9b88

Description: This video shows observations the specimens described in figures 1D, 1G, 1J and 1M using a confocal laser scanning microscope (βtubulin>GCaMP6s). GCaMP6s was confirmed to be expressed across a broad range of the nervous system extending from the PSN to the BV and MG.. Resource Type: Audiovisual. File: 260203_yes.mp4. DOI: 10.22002/pr70k-zht59

Description: This video shows observations the specimens described in figures 1E, 1H, 1K and 1N using a confocal laser scanning microscope (GCaMP6s). GCaMP6s was confirmed to be expressed across a broad range of the nervous system extending from the PSN to the BV and MG.. Resource Type: Audiovisual. File: 260325_GCaMP6s.mp4. DOI: 10.22002/8qp8v-6fx39

Description: This video shows observations the specimens described in figures 1E, 1H, 1K and 1N using a confocal laser scanning microscope (mCherry). mCherry was confirmed to be expressed across a broad range of the nervous system

extending from the PSN to the BV and MG.. Resource Type: Audiovisual. File: 260325_mCherry.mp4. DOI: 10.22002/dzedp-2cw40

References

Blondel VD, Guillaume JL, Lambiotte R, Lefebvre E. 2008. Fast unfolding of communities in large networks. DOI: 1742-5468/2008/10/P10008

Chen TW, Wardill TJ, Sun Y, Pulver SR, Renninger SL, Baohan A, et al., Kim DS. 2013. Ultrasensitive fluorescent proteins for imaging neuronal activity. Nature 499(7458): 295-300. PubMed ID: 23868258

de Felipe P, Luke GA, Hughes LE, Gani D, Halpin C, Ryan MD. 2006. E unum pluribus: multiple proteins from a self-processing polyprotein. Trends Biotechnol 24(2): 68-75. PubMed ID: 16380176

Donnelly MLL, Luke G, Mehrotra A, Li X, Hughes LE, Gani D, Ryan MD. 2001. Analysis of the aphthovirus 2A/2B polyprotein 'cleavage' mechanism indicates not a proteolytic reaction, but a novel translational effect: a putative ribosomal 'skip'. J Gen Virol 82(Pt 5): 1013-1025. PubMed ID: 11297676

Hamada M, Shimozono N, Ohta N, Satou Y, Horie T, Kawada T, et al., Satoh N. 2011. Expression of neuropeptide- and hormone-encoding genes in the Ciona intestinalis larval brain. Dev Biol 352(2): 202-14. PubMed ID: 21237141

Horie T, Shinki R, Ogura Y, Kusakabe TG, Satoh N, Sasakura Y. 2011. Ependymal cells of chordate larvae are stem-like cells that form the adult nervous system. Nature 469(7331): 525-8. PubMed ID: 21196932

Hozumi A, Horie T, Sasakura Y. 2015. Neuronal map reveals the highly regionalized pattern of the juvenile central nervous system of the ascidian Ciona intestinalis. Dev Dyn 244(11): 1375-93. PubMed ID: 26250096

Kanda T, Sullivan KF, Wahl GM. 1998. Histone-GFP fusion protein enables sensitive analysis of chromosome dynamics in living mammalian cells. Curr Biol 8(7): 377-85. PubMed ID: 9545195

Kusakabe T, Yoshida R, Ikeda Y, Tsuda M. 2004. Computational discovery of DNA motifs associated with cell type-specific gene expression in Ciona. Dev Biol 276(2): 563-80. PubMed ID: 15581886

Lenci S, Sieger D. 2025. Calciumnetexplorer: an R package for network analysis of calcium imaging data. BMC Bioinformatics 26(1): 220. PubMed ID: 40859128

Liu Z, Chen O, Wall JBJ, Zheng M, Zhou Y, Wang L, et al., Liu J. 2017. Systematic comparison of 2A peptides for cloning multi-genes in a polycistronic vector. Sci Rep 7(1): 2193. PubMed ID: 28526819

Miya T, Satoh N. 1997. Isolation and characterization of cDNA clones for beta-tubulin genes as a molecular marker for neural cell differentiation in the ascidian embryo. Int J Dev Biol 41(4): 551-7. PubMed ID: 9303342

Nguyen JP, Shipley FB, Linder AN, Plummer GS, Liu M, Setru SU, Shaevitz JW, Leifer AM. 2016. Whole-brain calcium imaging with cellular resolution in freely behaving Caenorhabditis elegans. Proc Natl Acad Sci U S A 113(8): E1074-81. PubMed ID: 26712014

Olivo P, Palladino A, Ristoratore F, Spagnuolo A. 2021. Brain Sensory Organs of the Ascidian Ciona robusta: Structure, Function and Developmental Mechanisms. Front Cell Dev Biol 9: 701779. PubMed ID: 34552923

Osugi T, Sasakura Y, Satake H. 2020. The ventral peptidergic system of the adult ascidian Ciona robusta (Ciona intestinalis Type A) insights from a transgenic animal model. Sci Rep 10(1): 1892. PubMed ID: 32024913

Ryan K, Lu Z, Meinertzhagen IA. 2016. The CNS connectome of a tadpole larva of Ciona intestinalis (L.) highlights sidedness in the brain of a chordate sibling. Elife 5: pii: e16962. 10.7554/eLife.16962. PubMed ID: 27921996

Schindelin J, Arganda-Carreras I, Frise E, Kaynig V, Longair M, Pietzsch T, et al., Cardona A. 2012. Fiji: an open-source platform for biological-image analysis. Nat Methods 9(7): 676-82. PubMed ID: 22743772

Sekiguchi T, Kawashima T, Satou Y, Satoh N. 2007. Further EST analysis of endocrine genes that are preferentially expressed in the neural complex of Ciona intestinalis: receptor and enzyme genes associated with endocrine system in the neural complex. Gen Comp Endocrinol 150(2): 233-45. PubMed ID: 17070810

Thompson JD, Higgins DG, Gibson TJ. 1994. CLUSTAL W: improving the sensitivity of progressive multiple sequence alignment through sequence weighting, position-specific gap penalties and weight matrix choice. Nucleic Acids Res 22(22): 4673-80. PubMed ID: 7984417

Totsuka NM, Hotta K. 2026. Optogenetic activation of primary sensory neurons induces metamorphosis in Ciona. Dev Biol 530: 77-85. PubMed ID: 41274435

Venkatachalam V, Ji N, Wang X, Clark C, Mitchell JK, Klein M, et al., Samuel AD. 2016. Pan-neuronal imaging in roaming Caenorhabditis elegans. Proc Natl Acad Sci U S A 113(8): E1082-8. PubMed ID: 26711989

Akahoshi T, Utsumi MK, Oonuma K, Murakami M, Horie T, Kusakabe TG, Oka K, Hotta K. 2021. A single motor neuron determines the rhythm of early motor behavior in Ciona. Sci Adv 7(50): eabl6053. PubMed ID: 34890229

Funding: This work was supported by the Global Science Campus program (Keio GSC) of the Japan Science and Technology Agency (JST).

Conflicts of Interest: The authors declare that there are no conflicts of interest present.

Author Contributions: Yuta Yoshino: writing - original draft, investigation, data curation, formal analysis, resources, visualization, methodology. Manami Doi: methodology, supervision, project administration, visualization, resources. Kohji Hotta: writing - review editing, supervision, conceptualization, funding acquisition.

Reviewed By: Anonymous

History: Received September 21, 2026 **Revision Received** October 14, 2026 **Accepted** November 6, 2026 **Published Online** November 10, 2026 **Indexed** November 24, 2026

Copyright: © 2026 by the authors. This is an open-access article distributed under the terms of the Creative Commons Attribution 4.0 International (CC BY 4.0) License, which permits unrestricted use, distribution, and reproduction in any medium, provided the original author and source are credited.

Citation: Yoshino Y, Doi M, Hotta K. 2026. βtubulin>GCaMP6s and βtubulin>H2B-GCaMP6s-T2A-mCherry enable pan-neuronal Ca^{2+}imaging and more accurate measuring neural activity in *Ciona robusta*. microPublication Biology. 10.17912/micropub.biology.002430